Research Article

Journal of Environmental Nanotechnology

Studies on $BaTiO_3$ Anode Material for Intermediate Temperature Solid Oxide Fuel Cell (IT-SOFC)

M. Rajasekhar*, N. Kalaivani, M. Nithya, J. Marimuthu
Government Arts College, Dharmapuri, TN, India
Received: 07.07.2016 Accepted: 23.08.2016 Published: 30-09-2016
*drmrchem@gmail.com

ABSTRACT

$BaTiO_3$ ($0 \leq x \leq 0.5$) nano crystalline powders were synthesized by $Ba(NO_3)_2$, $TiO(NO_3)_2$, and aspartic acid (fuel) in a combustion method with heating at 550 °C for 6 hours. This process remarkably reduced the synthesis time and less energy consumable to obtain $BaTiO_3$. The structure of $BaTiO_3$nano powders wereconfirmed by x-ray diffraction. The average crystallite size was determined from X-ray line broadening analysis by using the scherrer equation. The surface morphology of the synthesized product was observed by SEM studies. The formation of the product $BaTiO_3$was confirmed by FTIR studies. The synthesis and crystallization were followed by thermochemical techniques (TGA/DTA) studies. The synthesized materials showed reasonable electrical conductivity. These results indicates that assisted combustion method is a promising method to prepare nanocrystallite $BaTiO_3$ anode material for solid oxide fuel cell.

Keywords: Electrical conductivity, SEM, Scherequation, TGA & DTA, XRD and FTIR.

1. INTRODUCTION

Fuel cells are electrochemical device that converts the chemical energy of a directly into electrical energy.The electrochemical reactions take place at the electrodes to produce an electric current .Those presently under research development and demonstration generally use as fuel the H_2 and CO gas of a reformed hydrocarbon. Although the SOFC operates at a high temperature, it has several significant applications because it promises cleaner, more efficient energy conversional power plant or lower temperature polymer-based fuel cells .Targeted applications include the bottoming cycle of an electric power plant, domestic heat, power units and even electric vehicles. Stationary fuel cells are used for commercial, industrial and residential primary and backup power generation. Fuel cells are very useful as power source in remote locations, such as spacecraft remote weather stationary, large parks, communications centers, rural locations including research stations, and in certain military applications.

The anode material must be compatible (chemical and thermal expansion) with the electrolyte and provide means for transport of gas from the fuel, oxygen ions from electrolyte and electrons to the interconnect. The catalytic properties of the anode to the fuel oxidation reaction are also important, particularly as the operating temperature is decreased. The performance of a solid oxide fuel cell depends strongly on the anode structure which is mainly determined by fabrication method. In addition, electrochemical reactions are quite different from normal heterogeneous reactions in some aspects. Therefore, it is necessary to consider how to anode work on a microscope scale. It is well known that the electrochemical reaction can only occur at the three-phase boundary ,which is defined as the collection of sites where oxygen ion conductor (the electrolyte), the electron-conducting metal phase ,and the gas phase all meet together.

As a fuel arriving at the anode is a reducing agent, the anode can be made of metal. However, the material must not be oxidize during operation, thus limiting the cathode metals to nickel, cobalt and the noble metals. Nickel is most often used because of its low cost compared to the others. In order to enable flow of the fuel to the electrolyte, the anode must remain porous at the elevated operating temperature. Another requirement is to sufficiently minimize the mismatch in thermal expansion between the anode and electrolyte to maintain adhesion at the interface. These two requirements are achieved by dispersing the nickel within the solid electrolyte material to form a cermet.

Fuel cell systems have the advantage of being modular and can therefore be built in a wide range of power requirements from a few hundred watts up to multi-kilowatt and megawatt sizes. This range allows the construction of highly efficient power plants at specific locations. Long term planning, based on predictions of expected increased needs, can be more flexible and the early investment in over-sized systems can be avoided. Because of their low emission level, fuel cell power plants can be installed on-site, where energy is consumed, even in densely populated areas. As a result,

power transmission lines are more economic and transmission losses are reduced.

The basic principles of a fuel cell are those of the well-known electrochemical batteries, which are involved in many activities of our everyday life. The large difference is that, in the case of batteries, the chemical energy is stored in substances located inside them. When this energy has been converted to electrical energy, the battery must be thrown away (primary batteries) or recharged appropriately (secondary batteries). In a fuel cell, the chemical energy is provided by a fuel and an oxidant stored outside the cell in which the chemical reactions take place. As long as the cell is supplied with fuel and oxidant, electrical power can be obtained.

2. EXPERIMENTAL

The following chemicals were used for the synthesis of Bariumtitanate: Barium nitrate 99.99% (Sigma-Aldrich), TitaniumDioxide 99% (Sigma-Aldrich), Asparticacid. All the chemicals were analytical grade and used without further purifications. Deionized water was used as solvent for all the synthesis.

3. SYNTHESIS OF $BaTiO_3$

$BaTiO_3$ Powder was synthesized byassisted combustion method where and 0.39 g of $TiO(NO_3)_2$, dissolved in 2N nitric acid and mixed with 1.30 g of $Ba(NO_3)_2$ and 1.10 g of Aspartic acid in a beaker.Itwas then heated in a heating mantle at 80 °C until get gel liquid and finally foamy powder was obtained. The foamy powder was crushed and kept at 550 °C for 6 hours to get calcined powder of $BaTiO_3$. The yield was 90%.

The $TiO(NO_3)_2$ solution was prepared by following method. The 1.99 g of TiO_2 (AR grade), and 10 gram of ammonium sulphate (AR agar) were added to 80 ml of concentrated H_2SO_4 and the mixture was stirred on a hot plate until clear solution was obtained where Ti-oxy sulphate formed and then treated with ammonia at cold condition. The precipitated $TiO_2.XH_2O$ was filtered and washed free from the sulphate solution. This was treated with cold 1:1 nitric acid to get $TiO(NO_3)_2$ solution.

4. CHARACTERISATION

Powder X-ray diffraction patterns were recorded in the 2θ range of 20-80˚on a Philips X' pert X-ray powder diffraction using Cu Kα (λ=1.54178 A) radiation. Thermogravimetric analysis (TGA) was performed on Mettler-Toledo (TGA/DTA) in air at a heating rate of 10 °C /min. A scanning electron microscope (SEM) (Leo series 1430 VP) equipment with INCA was used to determine the morphology of samples. The FTIR measurement was carried out using a Agilent Cary 630 FTIR spectrometer in the range 400-4000 cm^{-1}. Thermogravimetric analysis (TGA) was performed on Mettler-Toledo (TGA/DTA) in air at heating rate of 10 °C/min.

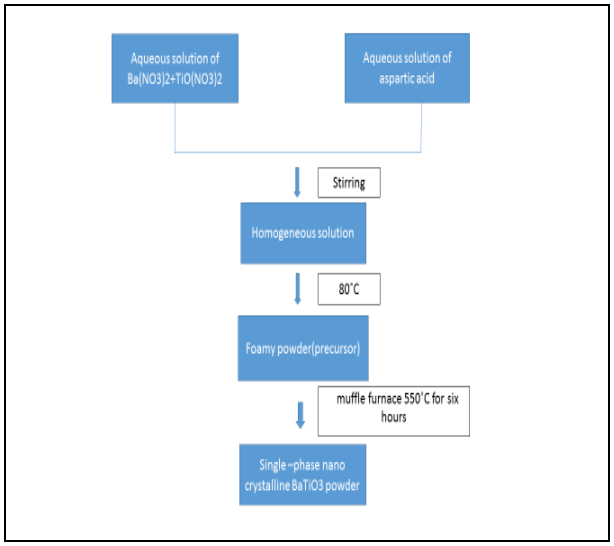

Fig. 1: Flow chart of assisted combustion synthesis of $BaTiO_3$

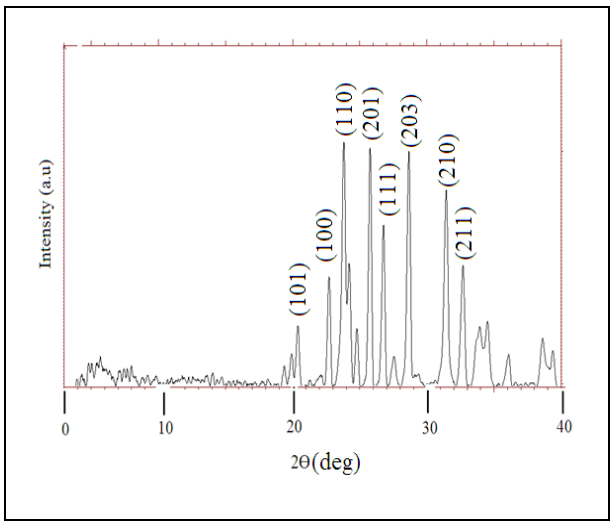

Fig. 2: X-ray diffraction pattern of $BaTiO_3$

5. RESULTS & DISCUSSION

5.1 X-ray Diffraction Studies

The powder XRD analysis was performed on the prepared $BaTiO_3$ nanocrystalline powders at 550 °C for 6 hours, significant 100, 110, 201, 111, 203, 210, and 211 planes of a cubic fluorite structure of $BaTiO_3$. The XRD pattern in the 2θ range of 30-40 showed presence of the (211) peak in synthesized material at low temperature .The peak broadening of an individual reflection decreases and become sharper with an increase in the reaction temperature, suggesting the increased crystallite. The average crystallite sizes of the $BaTiO_3$ particles

calculated from X-ray line broadening of the 110 diffraction using scherrer equation. It was in the range 3-15 nm. The crystallite size and lattice parameters calculated from XRD data. The lattice constant (a=6.8685Å, b=2.5961Å, and c=3.4343Å) and their lattice volume [61.2381Å] .indicates that the $BaTiO_3$ belongs to orthorhombic. It is identical with the sample prepared by conventional solid state method. The crystallite size of the $BaTiO_3$ is 32 nm.

5.2 SEM Studies

Fig. 3 shows the microstructure of $BaTiO_3$ powder obtained at the 550 °C for 6 hrs. The surface morphology of material in the form of Ortho rhombic structure and agglomeration were investigated with scanning electron microscope. The particle size was distribution for $BaTiO_3$ powders, the average grain size was 32 nm. The particles are uniformly distributed. There is agglomeration of the particles. The particles of the synthesized products are in nano range.

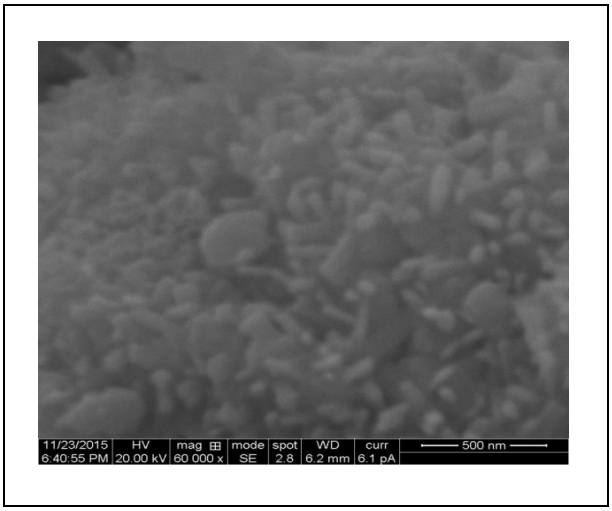

Fig. 3: SEM photograph of $BaTiO_3$

5.3 Particle Size Analysis

The average particle size of the prepared $BaTiO_3$was calculated from X-ray line broadening analysis using Scherrer equation

$$D = 0.9\lambda/\beta COS\theta$$

Where, D is the average particle size, λ is the wave length of Cu Kα radiation, β is the width (in radian) of the X-ray diffraction peak at half of its maximum intensity, and θ is the Bragg diffraction angle of the line. The average crystallite size values of $BaTiO_3$ nano powder obtained at 550 °C for 6 hours and it was 32 nm. The smaller average crystallite size (nanoparticles) was achieved by assisted combustion method compared to conventional solid state reaction method.

5.4 Differential Thermal Analysis (DTA) / Thermo Gravimetric Analysis (TGA)

In fig 4 shows that TGA/DTA pattern obtained on $BaTiO_3$ anode powder. In the TGA pattern the $BaTiO_3$ sample showed a weight loss of about 0.0464 mg/min until 65 °C. The sample on further heating from 65 °C - 335.97 °C, showed slight weight gain and loss of about 0.123mg/min. Again the sample showed a weight increase from 335.97 °C-560.53 °C and then a loss of 0.580mg/min during further heating up to 584.53 °C. The weight gain and weight loss indicated that the $BaTiO_3$ powder exhibited easy reversible absorbtion-desorbtion of oxygen from air.

From the DTA curve, it is seen that a broad exothermic peak at 586.83 °C occurred due to the weight losses between 39.95 °C-725.7 °C in TGA curve. From the above TGA/DTA data, the $BaTiO_3$ gradually absorbs the oxygen from air with temperature.

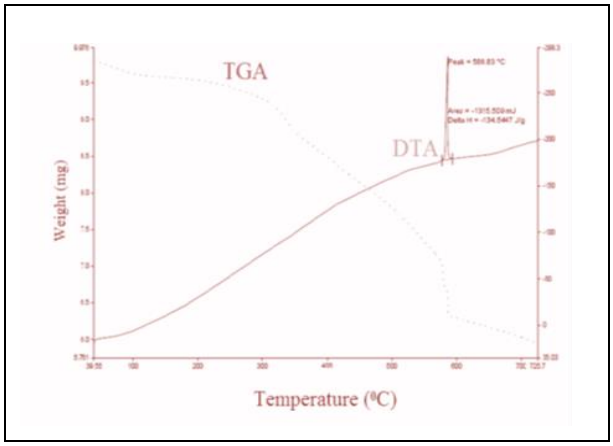

Fig. 4: TGA & DTA of $BaTiO_3$

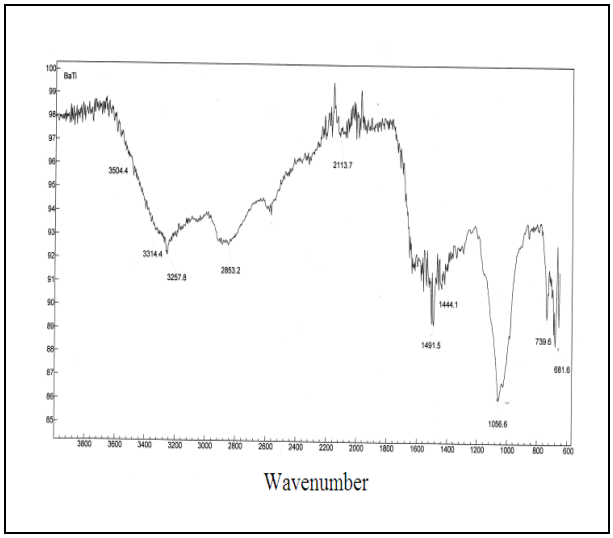

Fig. 5: FT-IR spectrum of $BaTiO_3$

5.5 Fourier Transform Infrared (FT-IR) Spectroscopy

Fig. 5 shows that the FT-IR Spectrum obtained on $BaTiO_3$ anode powder. The powder exhibited a strong bond at 600-800 cm^{-1} due to the stretching vibration mode of the Ba-O bond in the structure.

The peak appeared at 1491.5 cm^{-1} corresponds to the H-O-H bond mode confirming the presence of moisture in the sample. The peak appeared at 2113.7 cm^{-1} is due to the presence of CO_2in the sample. The sample $BaTiO_3$ exhibited a low intensity peak at 2600.09 cm^{-1}

The $BaTiO_3$ sample exhibited four peaks obtained between the wavelength region 2800-3800 cm^{-1} and are observed at 2853.2, 3257.8, 3314.4 and 3504.4 cm^{-1}. The peak appeared at 3257.8 cm^{-1} is related to the O-H stretching vibration of H_2O in the sample. The major peak reported for $BaTiO_3$ in literature coincide with the observed FT-IR spectrum for $BaTiO_3$ which confirmed the single phase of this anode material

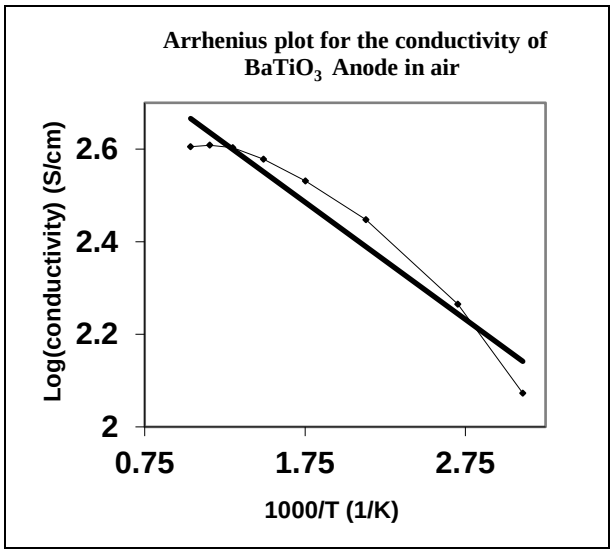

Fig. 6: Electrical conductivity of $BaTiO_3$

5.7 Electrical Conductivity

The Electrical Conductivity of $BaTiO_3$ was measured at temperature 100-700˚C in air is shown in fig 6. The $BaTiO_3$ Anode was a mixed conductor. The total conductivity involved both electronic and ionic conductivity terms, due to the presence of holes and oxygen vacancies. The ionic conductivity was about two orders of magnitude lower than electrical conductivity. The charge imbalance caused by a replacement of Ba^{2+} could be accommodated either by an oxidation of Ti^{4+} (electronic compensation) or by the formation of oxide ion vacancies (ionic compensation) in $BaTiO_3$. Electrical conductivity of $BaTiO_3$ increased gradually with temperature. For the composition with semi conducting behavior, the temperature dependence of the conductivity can be described by the small polaron hopping mechanism as $\sigma=A/T \exp(-Ea/KT)$ the activation energies obtained from the Arrhenius plots of log σ vs1000/T. The changes in the activation energy with temperature for $BaTiO_3$ are attributed to the spin state transition.

6. CONCLUSIONS

The present investigation was carried out to improve the performance of $BaTiO_3$ by the synthesis method. The electrochemical behavior of $BaTiO_3$ based anode materials depends upon the method of synthesis and sintering temperature. Hence, these conditions were adopted for the present work to synthesis the phase-pure, nanocrystallite materials. The present work was mainly focused on synthesis, and electronic conductivity of $BaTiO_3$.

FUNDING

This research received no specific grant from any funding agency in the public, commercial, or not-for-profit sectors.

CONFLICTS OF INTEREST

The authors declare that there is no conflict of interest.

REFERENCES

Jeffrey W., Fergus, Electrolytes for solid oxide fuel cells, J. Power Sources., 162(1), 30-40(2006). https://doi.org/10.1016/j.jpowsour.2006.06.062

Maheswari, D., Venkatachalam, P., Sol-Gel Synthesis and Characterization of TiO2 Nano Films in the Building of Dssc, J. Electron. Commun. Eng., 4(4), 29-33(2013).

Marcin R. Kosinski, Richard T. Baskar, Preparation and Property-Performance relationships in samariumdopedcerianano powders for solid oxide fuel cell electrolytes, J. power source, 196, 2498-2525 (2011).

Narorram Sutradhar ,Apurba Sinhamahapatra , Sandip Pahari , Muthirulandi Jayachandran, Balasubramanian Subramanian, Hari C. Bajaj and AsitBaran Panda, Facile Low-Temperature Synthesis of Ceria and Samarium-Doped Ceria Nanoparticles and Catalytic Allylic Oxidation of Cyclohexane, J. Phys. chem., 115, 7628-7637 (2011).

Orera, A. and Slater, P. A., New chemical Systems for Solid Oxide Fuel Cells, Chem.Mater., 22(3), 675-690 (2010). https://doi.org/10.1021/cm902687z

Osamu Yamamoto, Solid oxide fuel cells: fundamental aspects and prospects, Electrochimica Acta, 45, 2423-2435 (2000).

Rajasekhar, M., Subramania, A., Muzhumathi, S., Microwave-Assisted Combustion synthesis of nanocrystallineNdCoO3cathode material for intermediate temperature Solid oxide fuel cells (ITSOFCs) Application. J. Environ. Nanotechnol., 3(4), 64-67 (2014). https://doi.org/10.13074/jent.2017.09.173269